

Poster Reprint

ASMS 2023
Poster number ThP 520

Illuminating the Cellular and Molecular Response to Drug Treatment by Combining Bioenergetic Measurements with Untargeted Metabolomics

Mark Sartain¹, Genevieve C. Van de Bittner¹, Natalia Romero², Yoonseok Kam², Maria Apostolidi¹, Dustin Chang¹

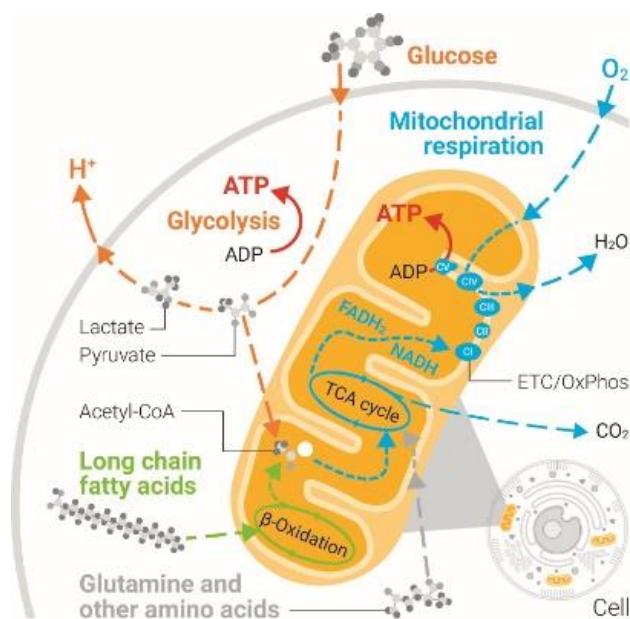
¹Agilent Technologies, Inc., Santa Clara, CA, USA

²Agilent Technologies, Inc., Lexington, MA, USA

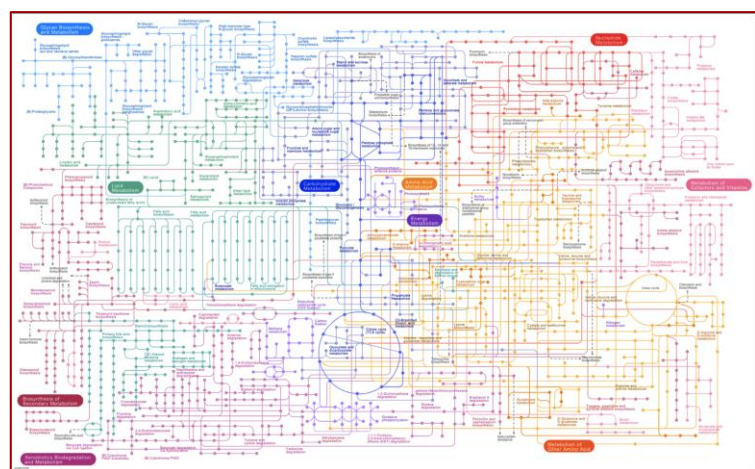
To better understand the biology of cancer cells and their dynamic metabolic response to therapeutic compounds, advanced methodologies are required. We combined results from two technologies that measured metabolic pathway utilization at two scales, cellular and molecular. An acute monocytic leukemia cell line was treated with the drugs SU1498 and AG-879, which were selected from a library of 80 kinase inhibitors based on their modulation of mitoATP production rates. Separately, cells treated with the drugs were lysed, metabolism was quenched, and metabolites and lipids were extracted with an automated sample preparation method. Extracts were directly analyzed with LC/Q-TOF and discovery-based MS software. The combined results provided deeper insight into the cellular and molecular metabolic response to drug treatment.

Seahorse XF analyses provide measurements at a cellular resolution

Cellular oxygen consumption and extracellular acidification rates



LC/MS omics and qualitative flux analyses provide measurements at a molecular resolution



Production and consumption of individual metabolites, lipids and proteins

Sample Preparation

THP-1 cells were cultured in supplemented RPMI medium and treated with SU1498, AG-879, or DMSO vehicle for either 1-2 hours (Seahorse XF) or 18 hours (XF and LC/MS). Cells were stained for viability assessment and counted for sample normalization with an Agilent Novocyte Quanteon flow cytometer. Kinetic measurements were made with the Agilent Seahorse XF Real-Time ATP Rate Assay to determine ATP production rates specific to glycolysis and mitochondrial respiration as well as the Mito Stress Test for a deeper investigation of drug impact on mitochondrial respiration rates. For LC/MS, metabolites were extracted with an automated dual metabolite + lipid extraction process with an Agilent Bravo Liquid Handling Platform using a supplementary protocol.¹ Metabolite extracts were separated with HILIC-LC and analyzed with an Agilent Revident LC/Q-TOF. Datasets were analyzed with Agilent MassHunter Explorer software.

Workflow Overview

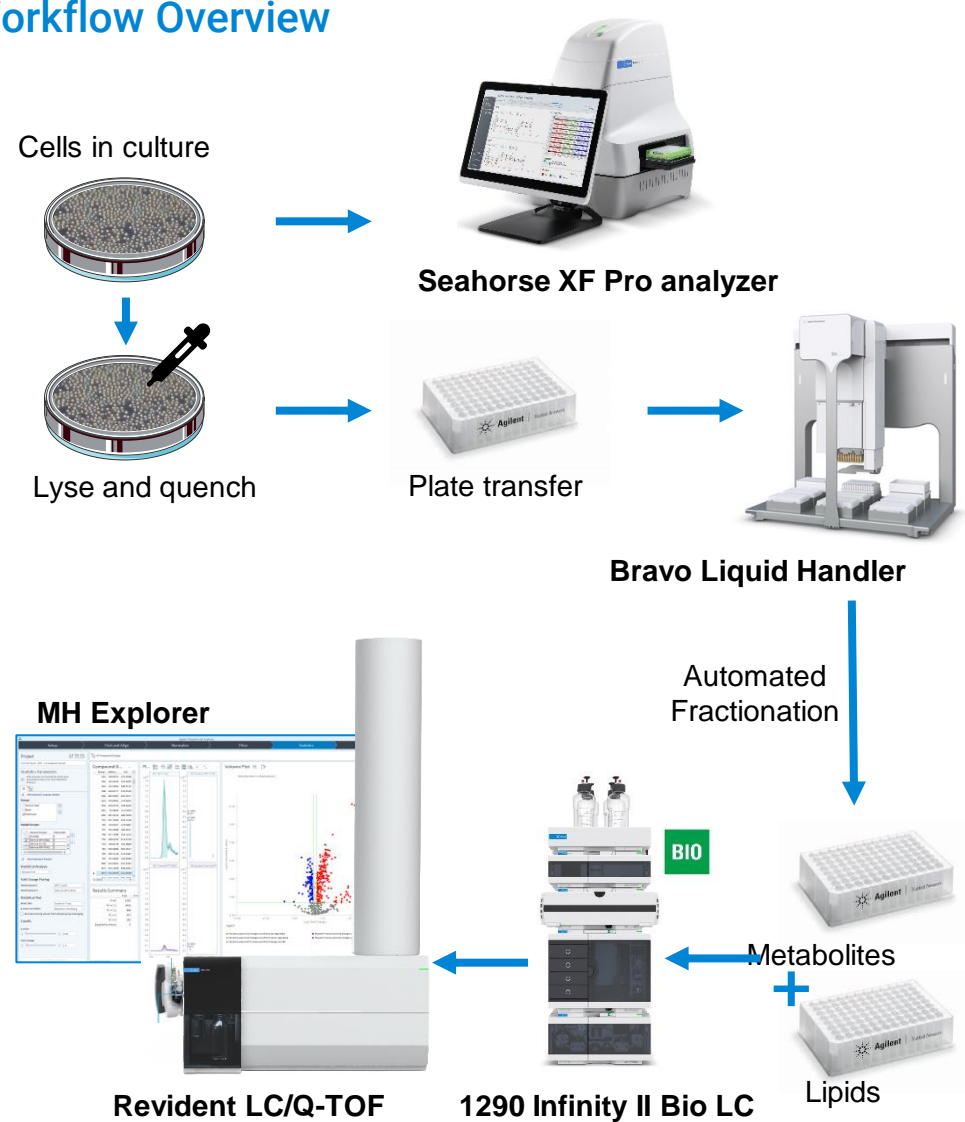


Figure 1. Overview of workflow, from cell culture to Seahorse XF and from cell culture to automated sample preparation to LC/MS analysis.

Tyrosine Kinase Inhibitor Screen Identifies Compounds of Interest

A kinase inhibitor library was screened with the Agilent Seahorse XF Real-Time ATP Rate Assay to assess acute effects of the inhibitors on mitochondrial ATP production rates.² Two inhibitors, AG-879 and SU1498, were selected for additional XF and LC/MS analysis, and MitoATP production rate IC₅₀ values were determined.

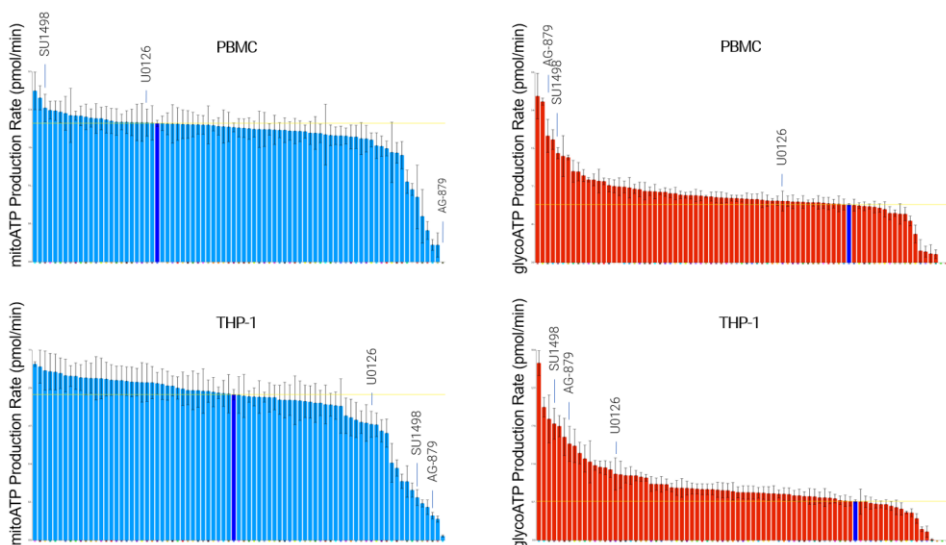


Figure 2. Effect of 80 kinase inhibitors on mitoATP production rate in THP-1 and PBMC cells. AG-879 reduced mitoATP production rates in both THP-1 cancer cells and healthy PBMCs. SU1498 reduced mitoATP production rates in THP-1 cells, but not in healthy PBMCs.

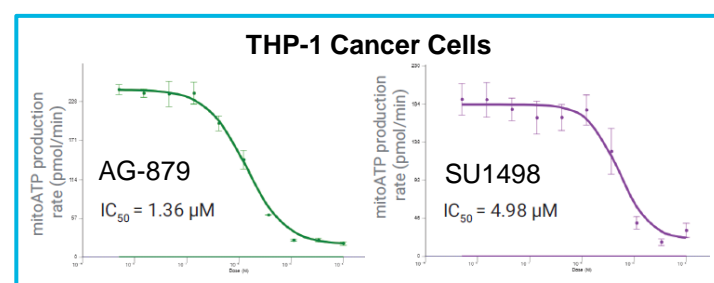


Figure 3. MitoATP production rate dose response curves and IC₅₀ values.²

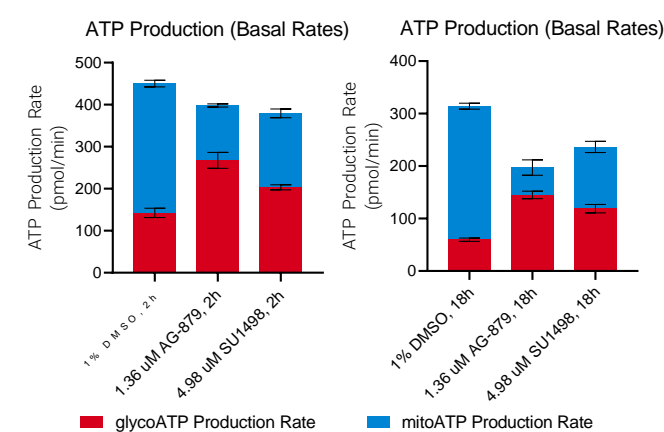


Figure 4. IC₅₀ AG-879 and SU1498 doses increase glycoATP and decrease mitoATP production rates after 2h and 18h. Total ATP production rates decrease relative to vehicle control after 18h with AG-879 or SU1498.

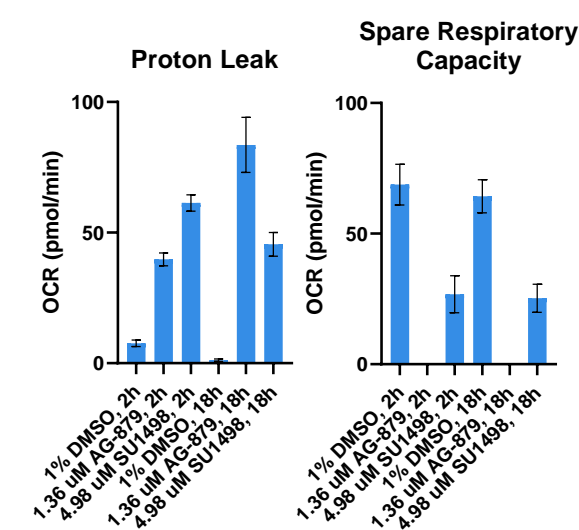


Figure 5. AG-879 and SU1498 increase proton leak by uncoupling oxygen consumption from mitoATP production. AG-879 induced proton leak increases from 2h to 18h of treatment, while SU1498 induced proton leak decreases from 2h to 18h (ANOVA). SU1498 reduces spare respiratory capacity (SRC); AG-879 causes complete loss of SRC.

Untargeted Metabolomics (Mx)

HILIC(-) LC/Q-TOF datafiles were processed in MH Explorer software. Metabolite annotations were made using an AMRT search with a subset of the Agilent METLIN PCDL curated with HILIC-Z retention times.

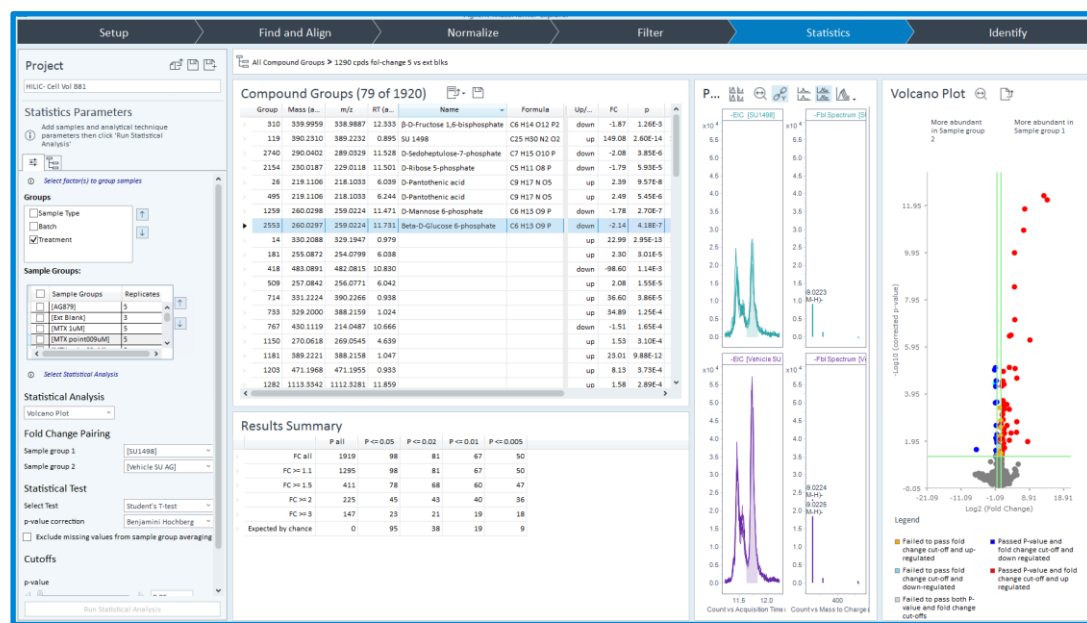


Figure 6. MH Explorer UI showing statistical analysis of HILIC(-) SU1498 treatment versus control samples, with 79/1920 compounds passing significance thresholds. Shown are results for glucose-6-phosphate. Cut-offs: Fold-change >1.5 and p-value <0.05.

Analysis based on the HILIC(-) dataset indicate similar trends for both drug treatments with a smaller magnitude of change for AG-879. Both drugs resulted in a decrease of sugar phosphates, intermediates in glycolysis that may correlate to the increased glycoATP production rate observed in Fig. 4. Conversely, pantothenic acid, a precursor for acyl-CoA required for pyruvate metabolism in the TCA cycle, was increased with SU1498 treatment, which may correlate with the XF measured reduction in mitoATP production.

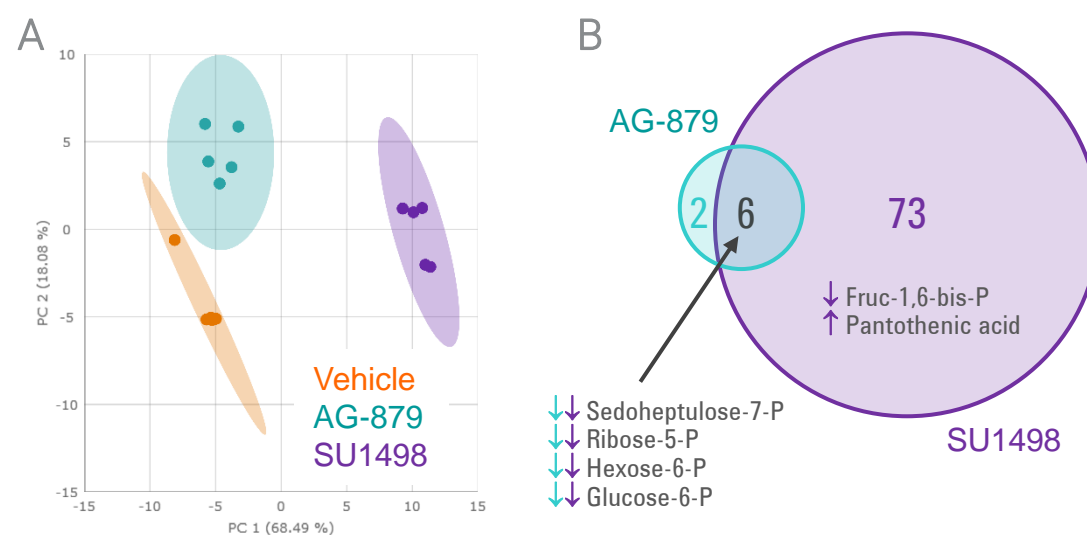


Figure 7. (A) Supervised PCA based on HILIC(-) significant compounds for AG-879 and SU1498 versus vehicle control. (B) Venn Diagram of significant compounds with compound annotations. Direction of arrows indicate significant increase (↑) or decrease (↓) relative to vehicle control.

Untargeted Lipidomics (Lx)

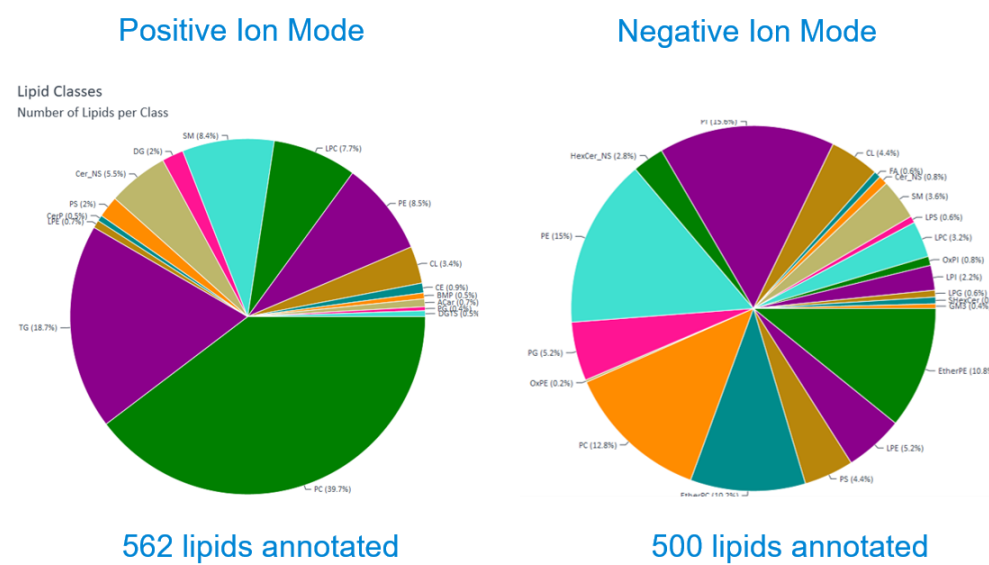


Figure 8. Agilent Lipid Annotator software results from 2 sets of 6 iterative MS/MS datafiles acquired on pooled THP-1 cellular lipid extracts prepared with the dual automated workflow.

Lipid Annotator results from Fig. 8 were used in MH Explorer for an AMRT database search. A third curated database³ leveraging the same chromatography⁴ was additionally used resulting in 677 lipid annotations out of 4,476 compounds in the positive-ion mode project (right).

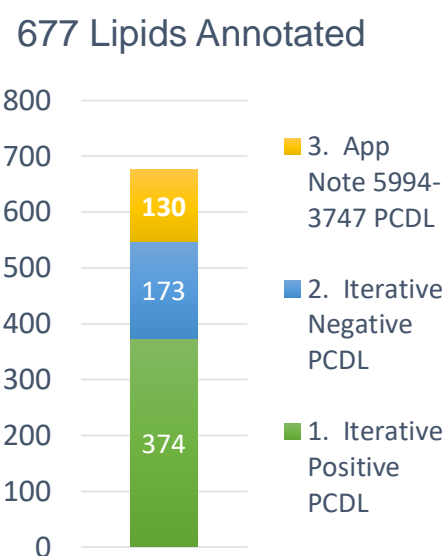


Figure 9. (A) MH Explorer PCA based on 677 annotated lipid compounds. Volcano plots of AG-879 (B) and SU1498 (C) versus vehicle control. 95 significant lipids are shown for the latter, with significant classes noted (Cer_NS, ceramides; TGs, triacylglycerols; CE, cholesterol esters).

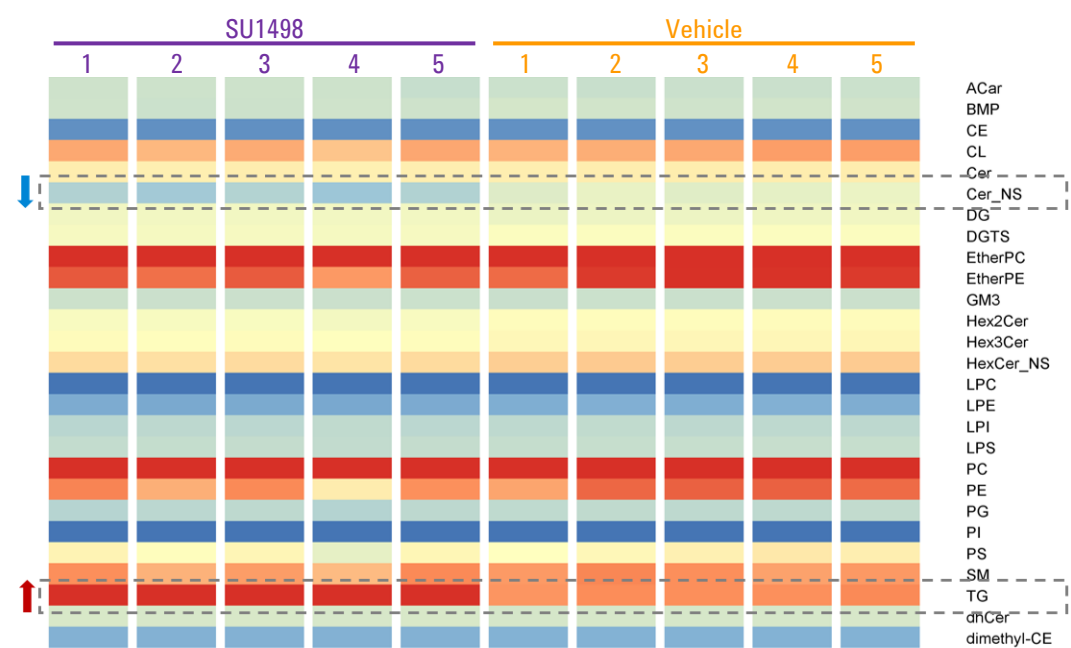
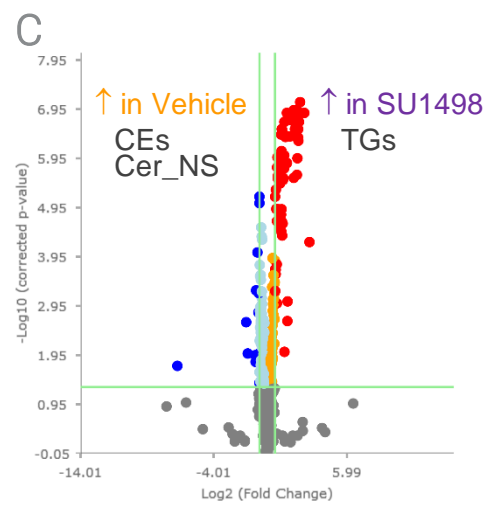
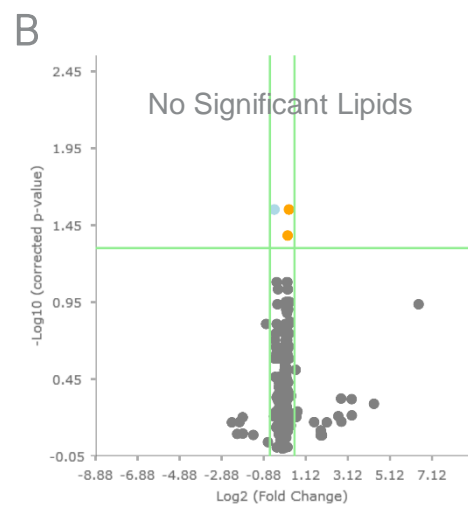
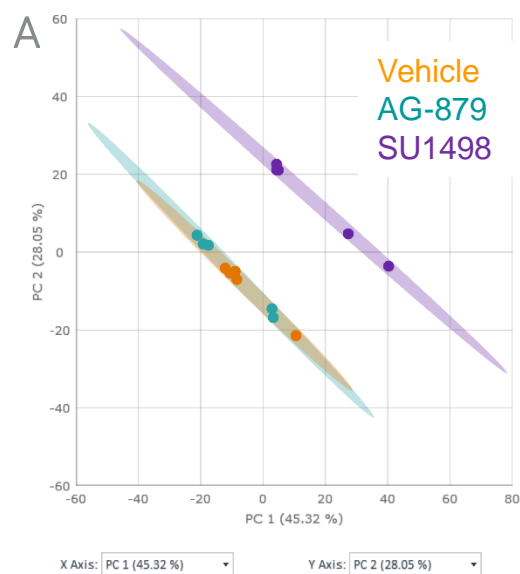


Figure 10. Lipid Class matrix plot in MPP created from exported MH Explorer .pfa results. Notable differences in ceramide (Cer_NS) and triacylglycerol (TG) classes are highlighted.

Conclusions

Combining XF and LC/MS technologies provided deeper insight into the cellular and molecular metabolic response to drug treatment for cancer research.

- XF analysis of AG-879 and SU-1498 corroborated previous results² and newly demonstrated that both drugs cause mitochondrial uncoupling.
- Untargeted Mx identified changes in key metabolites affected in glycolysis and mitochondrial respiration that correlate with XF results.
- Untargeted Lx showed an increase in TG content with SU-1498 treatment which may be related to buildup of energy precursors for the TCA cycle, shown to be reduced with XF.
- Future directions could include 1) further mining of the unidentified significant features, 2) qualitative flux analysis, and/or 3) the Seahorse XF Substrate Oxidation Stress Test to assess fuel dependencies with drug treatment.

References

- ¹ Van de Bittner, GC et al. An Automated Dual Metabolite + Lipid Sample Preparation Workflow for Mammalian Cell Samples. Agilent Technical Overview 5994-5065EN, 2022.
- ² Kam, Y et al. Rapid Bioenergetic Functional screening of Anticancer Drug Candidates. Agilent Application Note 5994-5651EN, 2023.
- ³ Mohsin, S, et al. High confidence targeted data mining of untargeted high-resolution data for lipids in plasma. ASMS Poster MP 463, 2023, Houston, TX
- ⁴ Hyunh, K et al. A Comprehensive, Curated, High-Throughput Method for the Detailed Analysis of the Plasma Lipidome. Agilent Application Note 5994-3747EN, 2021.

<https://www.agilent.com/en/promotions/asms>

This information is subject to change without notice.

For Research Use Only. Not for use in diagnostic procedures.

RA45069.5625810185

© Agilent Technologies, Inc. 2023
Published in USA, May 31, 2023